Analysis of a Photovoltaic System: AC and DC Power Quality

DANIELE GALLO[1], CARMINE LANDI[1], MARIO LUISO[1], EDOARDO FIORUCCI[2]

[1]Department of Industrial and Information Engineering
Second University of Naples
Via Roma 29, 81031 Aversa (CE)
ITALY
{daniele.gallo, carmine.landi, mario.luiso}@unina2.it

[2]Department of Electrical and Information Engineering
University of L'Aquila
Via G. Gronchi 18 – Pile, 67100 L'Aquila
ITALY
edoardo.fiorucci@univaq.it

Abstract: - Since the penetration of photovoltaic systems in the electrical network is increasing, the need to register and model the contribution of these energy sources, in terms of generated disturbances, quality and amount of available power, is becoming a crucial issue for optimal management of grid. So, this paper, starting from data experimentally recorded on a medium scale photovoltaic system that is grid connected, performs a certain number of analyses both in AC and DC side, in order to better understand and explore the nature of electricity generation patterns of PV plants. In addition to the calculation and the comment of common steady state power quality indexes, also transitory situations are analyzed and discussed. Finally, an analysis of the electric power components according IEEE 1459 is performed and the results show that the application of that standard in this practical case presents some critical aspects.

Key-Words: - voltage measurement, current measurement, power measurement, power quality measurement, photovoltaic plant, IEEE 1459.

1 Introduction

The use of photovoltaic (PV) systems is becoming wide in many countries as a result of active government policies for renewable energy sources. This trend arouses much concern on the current and voltage distortion caused by the power electronics used by these systems. Some issues that arise from the use of PV generation are as follows: 1) the disturbance behavior of these distributed resources and their relation with the weather variations and the nominal output current of the PV systems; 2) the acceptable penetration level of PV systems in the LV distribution network without disturbance limits, posed by the standards ([1]-[3]) being exceeded.

Moreover, one of most important issues in the analysis of a renewable generation systems are the quantification of the amount and the quality of energy that is in injected into the electrical grid, at least for revenue purposes. Despite of the economic importance of this aspect, the evaluation of power and energy flows in non-sinusoidal and unbalanced conditions is still one of the most complex aspects of metrology and in scientific literature, there is still not a full agreement in definitions, measurement methodologies and result interpretation ([4]-[7]). A big contribution in this field comes from the IEEE 1459 standard [4]. This standard includes definitions for the measurement of electric power quantities under sinusoidal, nonsinusoidal, balanced, or unbalanced conditions. The introduction of the IEEE Standard 1459 states that "the new definitions were developed to give guidance with respect to the quantities that should be measured or monitored for revenue purposes, engineering economic decisions, and determination of major harmonic polluters". The analysis of nonsinusoidal electrical systems has preeminent importance in renewable system due to their nonlinear or time varying behavior of the

power devices related with energy injection into the electrical grid.

This paper presents the results of the analysis of data acquired during a measurement campaign performed on June 2011 in a 20 kW PV plant in Avellino (in Southern Italy) [8]. This analysis aims to capture the electrical behavior of the PV plant ([9]-[32]), in order to better understand and explore AC and DC power quality (PQ) issue related with PV plants large diffusion. In addition to analysis of main steady state PQ indexes, also the analyses of some transient events are performed. Finally, an analysis of the electric power components according to IEEE 1459 is conducted. The aim is to provide useful data and some insights to explore the possibility of a better use of renewable energy sources.

2 The measurement campaign

2.1 Description of the site
The PV station studied in this work is a system, with peak power equal to 19.82 kW, located in Avellino, in the south of Italy. The station is installed on a portion of a flat roof of an industrial plant: it is a new installation operating since November 2009 and it is directly connected to the low voltage distribution system, without isolation transformer. It consists of six strings and two 10 kW three-phase inverters, each one having two DC inputs with separate maximum power point trackers (MPPT). For each inverter, at one input one single string is connected and at the other input the parallel of two strings is connected. The strings are made by panels having powers of 200 W, 210 W and 220 W. In Table I the main specifications of the PV station are summarized. More details are in [8] together with some additional results of simple analysis that are here not recalled here for sake of brevity.

2.2 Instrumentation
In the measurement campaign, direct current (DC) and alternate current (AC) electrical quantities and solar irradiance have been measured (see Fig. 1). The solar irradiance has been measured through a pyranometer. It is composed by a radiometer and a pyranometric probe. The radiometer is the Delta Ohm HD 2302.0: it measures illuminance, luminance, PAR (Photosynthetically Active Radiation) and irradiance depending on the connected probe. The used probe is the LP PYRA 02 whose main characteristics are sensibility of 10 $\mu V/(W/m^2)$, measurement range of $0 \div 2000$ W/m^2 and nonlinearity $<|\pm 1|\%$.

Table 1. Main specifications of the PV station.

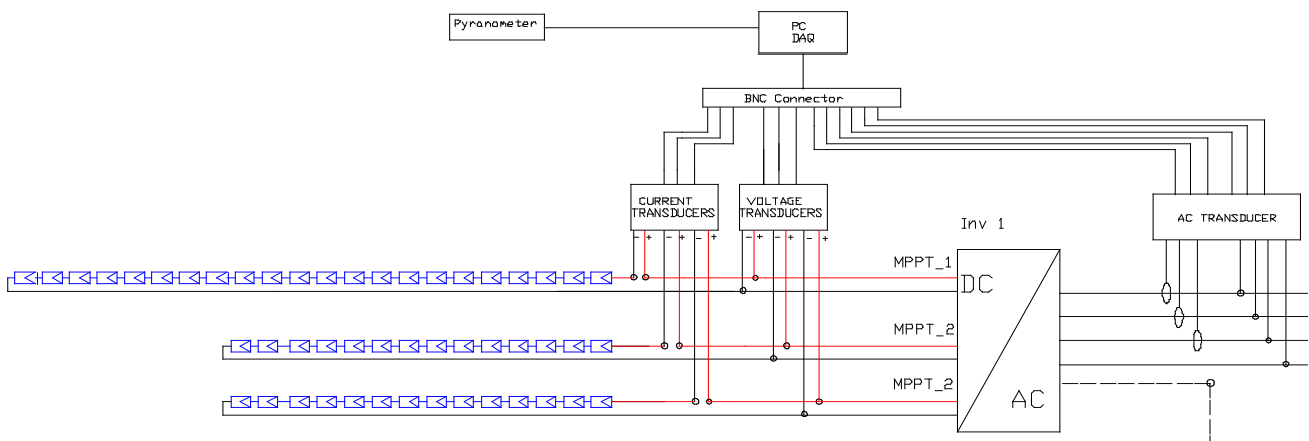| Inverter/ MPPT		Number of panels	Peak Power [kW]	Rated Voltage [V]	Open Circuit Voltage [V]	Rated Current [A]	Short Circuit Current
1	MPPT 1	22	4.4	589	683	7.5	8.0
	MPPT 2	14	2.9	422	510	7.0	7.5
		14	2.9	422	510	7.0	7.5
2	MPPT 1	14	2.9	422	510	7.0	7.5
	MPPT 2	15	3.3	459	553	7.0	7.7
		15	3.3	459	553	7.0	7.7

Fig. 1. Positioning of the measuring instruments

Regarding the electrical measurements, the paper focuses only on the electrical quantities related to Inverter 1, indicated in Table 1. In particular, the three DC voltages and the three DC currents of the three input strings of Inverter 1 and the three AC output voltages and the three AC output currents of the Inverter 1 have been measured and analyzed in the following. The measurement of AC and DC electrical quantities has been performed through a specifically built instrument. It is composed by a personal computer (PC), a data acquisition board (DAQ) and voltage and current transducers (see Fig. 1). The DAQ has 16 analog inputs, resolution of 16 bit, maximum sampling frequency of 250 kHz, input range of ±10 V. Six VT and six CT have been used: all the voltages have been sensed through LEM CV3-1000, three DC currents through LEM CT-10 and three AC currents through Fluke i400. The waveforms both at AC and DC side have been sampled at frequency of 10 kHz and stored in memory. The measurement software has been made in LabVIEW environment.

3 AC Steady State Power Quality Analysis

In this subsection some main results of AC power quality analysis performed through calculations of main steady state indexes during a full shining sunny day are reported. Fig.2 shows the reactive power as function of the active power at the fundamental frequency. As it results, for the considered PV system it is quite proportional to the active power, with a proportionality factor equal to -18 VAR/kW thus the plants at fundamental frequency behaves as ideal source with a nearly unitary power factor. Fig.3 shows voltage total harmonic distortion (THDV) as function of active power: it is practically not correlated with system output power, as expected for power level of considered system. As expected, it can be seen from Fig.4 that, when the active power is low the current total harmonic distortion (THDI) is very high, reaching values as high as 190 % in all AC lines. This situation can be better understood from Fig.5 where THDV is shown as function of THDI: THDV clearly increases when THDI increases. THDI is high for low active power because in such situation the inverter does not work in its nominal operating conditions generating high distorted current waveform. It is worthwhile underlining that this is a normal working condition for PV system at certain time of the day (f.i. sunrise and sunset). So at that times of the day, power systems with large

penetration of PV generation system are expected to be subjected to high harmonic pollution. Fig.6 shows voltage unbalance as function of active power: the two quantities are uncorrelated as unbalance comes from supply network. Fig.7 shows current unbalance as function of active power: it is very high at low active power value. Probably this is due to control strategy that, in order to maximize single line power, adopts an asymmetrical injection. Fig.8 and Fig.9 show respectively the maximum and mean values of voltage and current harmonic groups ([24]) at low frequency (50-2500 Hz) measured over the whole day. The reported values refer to the first phase but the other phases have, in this range, similar amplitudes. Voltage harmonics have remarkable amplitudes at the 3rd, the 5th and the 11th order; anyway corresponding current harmonics have low values indicating that this pollution is not induced by PV system but comes from supply network.
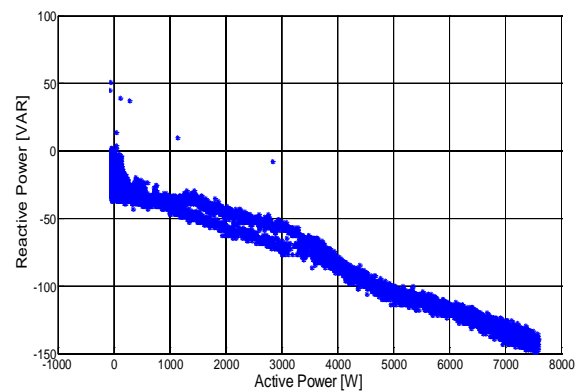

Fig. 2. Reactive power versus active power at the fundamental frequency.
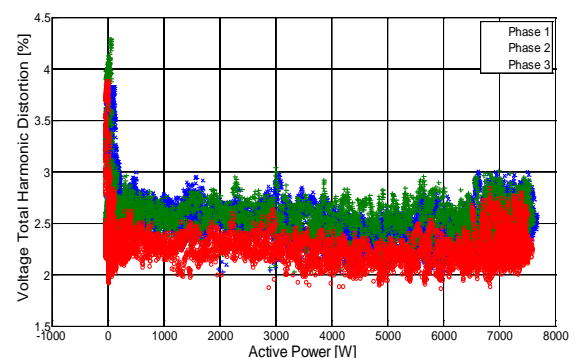

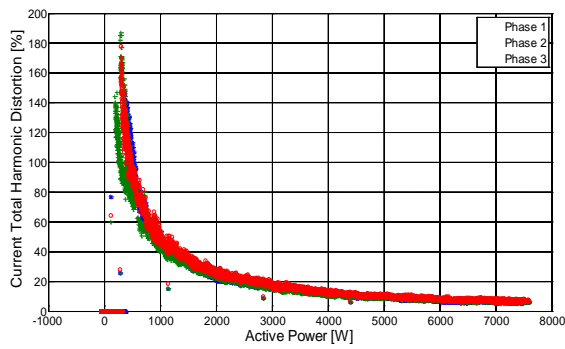Fig. 3. Voltage total harmonic distortion versus active power.

Fig. 4. Current total harmonic distortion versus active power.

The 11th harmonic has high value both in voltage and current: reasonably this component is induced in the voltage by current generate by PV system. This fact is particularly interesting: the system impedance can be evaluated at the 11th order harmonic could give useful information about the network status [12]. It is interesting to analyze the spectra over a wider frequency range till reaching the maximum value analyzable by considered acquisition system: 10 kHz.
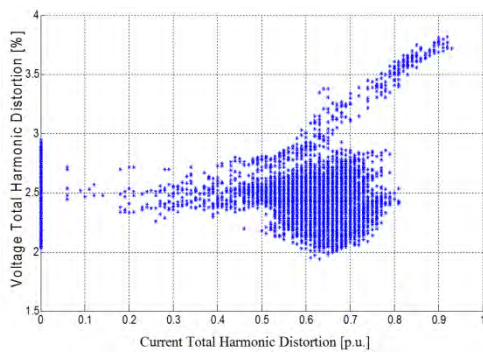
Fig. 5. Voltage THD versus Current THD.
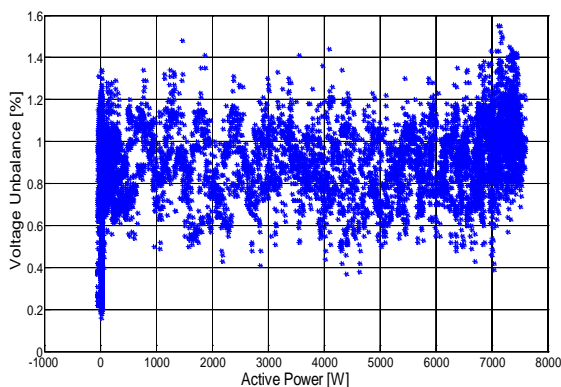
Fig. 6. Voltage unbalance versus active power.
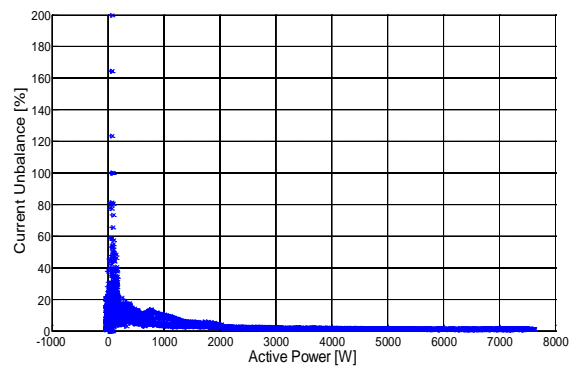
Fig. 7. Current unbalance versus active power.
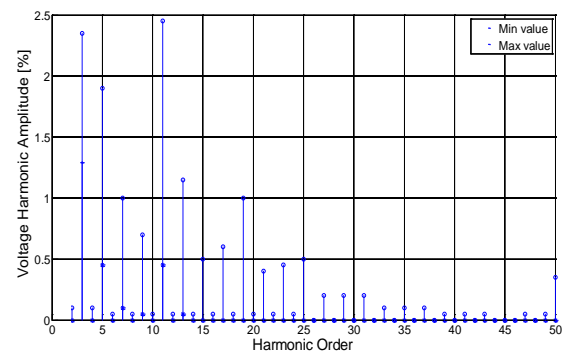
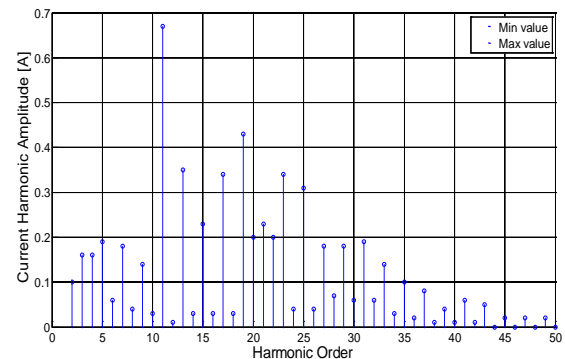Fig. 8. Minimum and maximum values of voltage harmonics over the three lines.

Fig. 9. Minimum and maximum values of current harmonics over the three lines.

In Fig. 10 and Fig. 11 the maximum values for harmonic groups ([24]) measured over the whole day are reported. In the current spectrum, it is apparent that the high switching frequency of inverter shifts at high frequency the most important spectral components that are, in this way, out of the common range adopted for basic THD analysis in agreement with standard (below 3 kHz [3], [24]).

These components, even reaching remarkable amplitude, have anyway a limited impact on system voltage.

4 AC Power Analysis according IEEE 1419

In this section, an analysis of the amount and the quality of energy that is in injected into the grid is performed, with reference to definitions contained in [4]. All the graphs reported in this paragraph have been depicted with values continuously calculated over a time windows of two seconds.
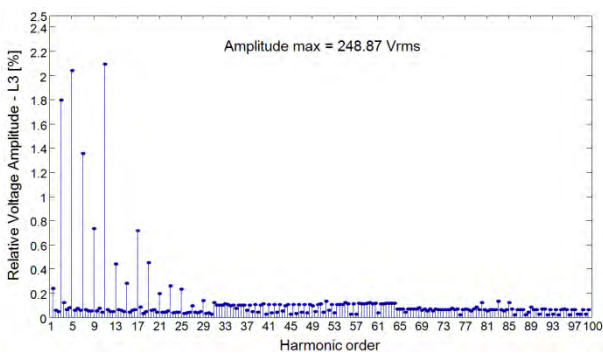

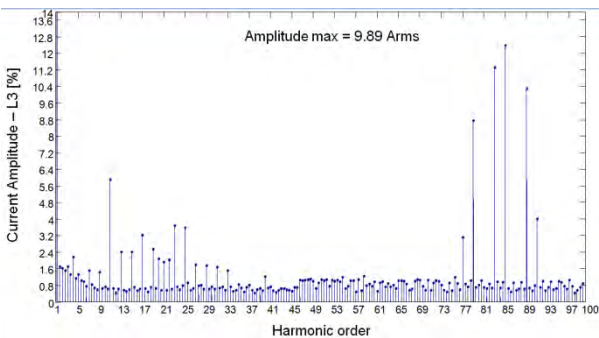Fig. 10. Wide frequency maximum values of voltage harmonics.

Fig. 11. Wide frequency maximum values of current harmonics.

Fig. 12 reports total active power and apparent power measured in time domain. While active power has a behavior like what was expected for this kind of system, it is evident a remarkable unforeseen oscillation in the apparent power that is preeminent especially at the beginning and at the end of the production.

In order to make this oscillation more evident a zoom of fig. 12 is reported in fig. 13. After a certain time from the start of the operation of the inverter

(highlighted in the Fig. with a vertical line), the apparent power starts to oscillate with a peak to peak value of about 900 VA with a period of about 40 second. It is useful to analyze this oscillation calculating nonactive power ([14]) as follows:

$$N = \sqrt{S^2 - P^2} \tag{1}$$

Fig. 14 shows that oscillation keeps nearly constant in amplitude and frequency for all the time in which inverter injects power into the grid. In order to analyze the source of this oscillation, it could be useful to decompose the apparent power into its components:

$$S^2 = P_1^2 + Q_1^2 + D_I^2 + D_V^2 + S_H^2 \tag{2}$$

where P_1 and Q_1 are active and reactive power at system frequency, D_I and D_V are current and voltage distortion power and S_H is the harmonic apparent power (see [14]).
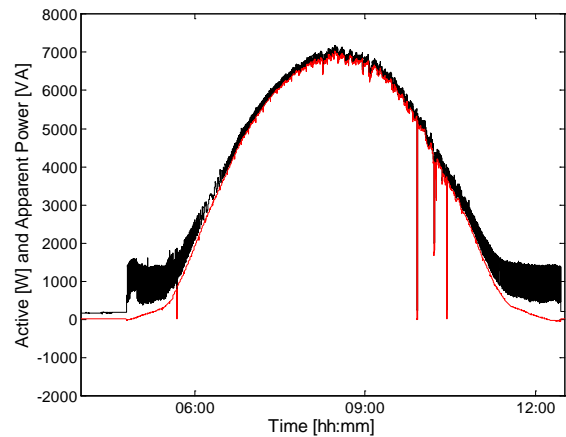

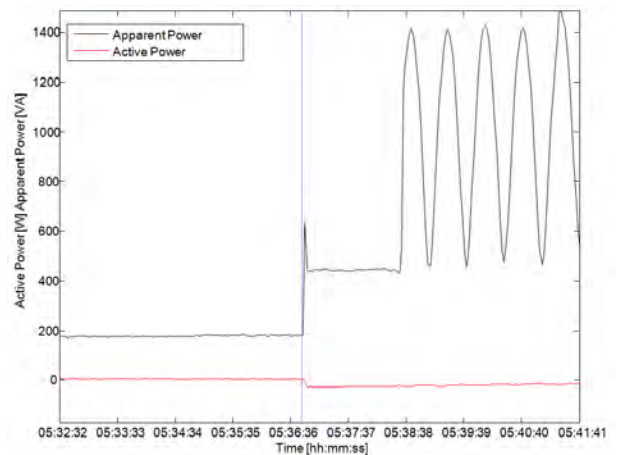Fig. 12. Active and Apparent Power versus time.

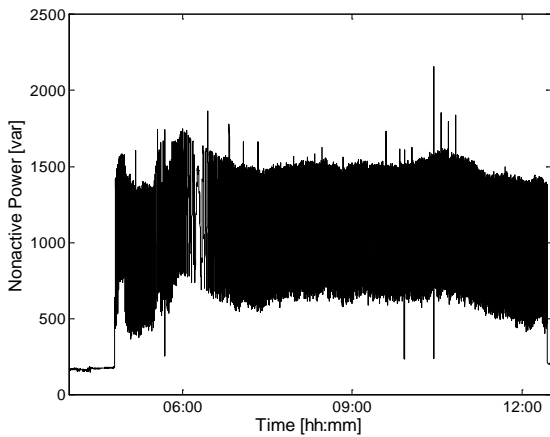Fig. 13. Zoom of Active and Apparent Power versus time.

Fig. 14. Non Active Power versus time.

Since

$$S_H^2 = P_H^2 + D_H^2 \tag{3}$$

and

$$P^2 = P_1^2 + P_H^2 \tag{4}$$

it results

$$N^2 = S^2 - P^2 = Q_1^2 + D_I^2 + D_V^2 + D_H^2 \tag{5}$$

So, one of these terms should oscillate in agreement with Fig. 14. But, these power components are reported from Fig. 15 to fig.18 and none of them can justify the nonactive power behavior. So we miss something. Deepening the investigation, we discovered that the oscillation comes from AC current, as it is apparent from Fig. 19 where the instantaneous values of AC current of first line are reported during one minute at about 5:40 AM. Similar behavior was found on the other lines but not reported here for sake of clarity. The sources of the oscillation are time varying spectral components at high frequency as it can clearly be seen comparing high resolution spectrum calculated over corresponding time samples taken from first time second (Fig. 20a) and last second (Fig. 20b) of the current in fig. 19. They come from switching behavior of the inverter and are forecasted. The problem is that these components should be included in D_H and D_I producing considerably higher values for these power components. In addition their amplitude is expected to oscillate in a way similar to that of fig. 14 as a consequence of their time varying behavior. But none of these effects apply. The reason for what found comes from a closer look to these high frequency components that reveal not to be harmonics. In fact, the four higher peaks reported in Fig. 20b measured with high resolution by spectral interpolation [25] are at 3945 Hz, 4145 Hz, 4245 Hz, 4445 Hz while fundamental component measured on line voltage

was 50.006 Hz: fluctuating components are interharmonics that are not included in definitions reported in [4].
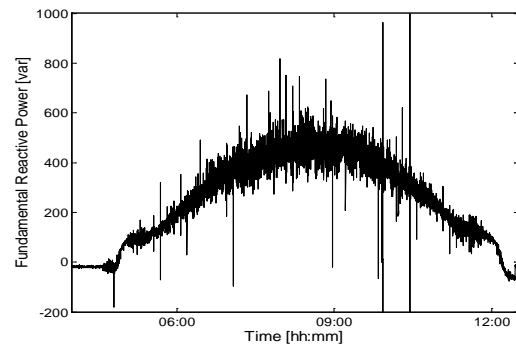

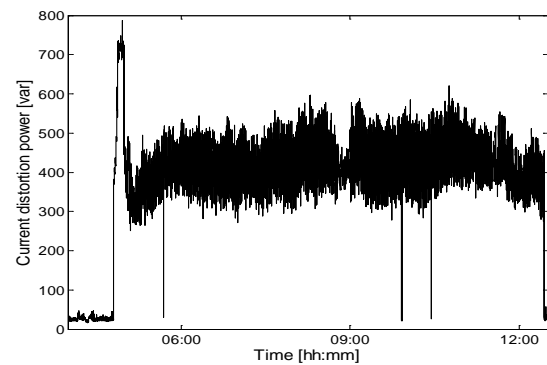Fig. 15. Fundamental Reactive Power versus time.

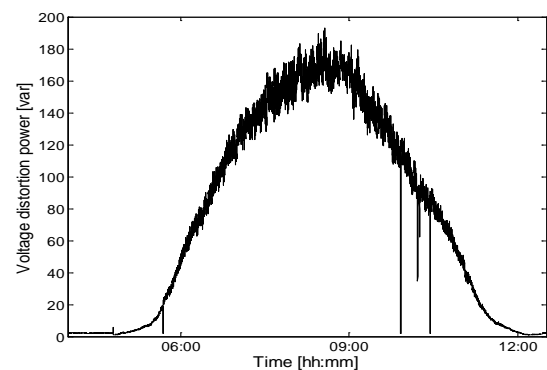Fig. 16. Current Distortion Power versus time.

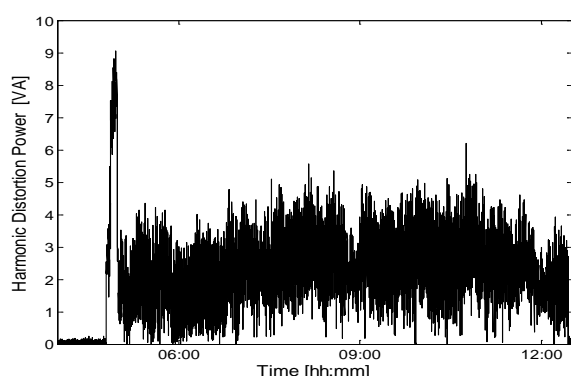Fig. 17. Voltage Distortion Power versus time.

Fig. 18. Harmonic Distortion Power versus time.

A comprehensive analysis of this problem is beyond the aim of this paper but it appears to be a big limit of IEEE standard and further analyses of this issue will be performed in future works.

As final remarks, it is worthwhile noting that spectrum in Fig. 19 is coherent with that in Fig. 20, which reports harmonic groups, calculated in agreement with [24]. These groups include spectral components that are closer than 5 Hz to harmonic positions, so that interharmonic components found in Fig 19 through an high resolution spectral analysis are included in nearer harmonic group of Fig. 20, that are the result of a low resolution (5 Hz) analysis.
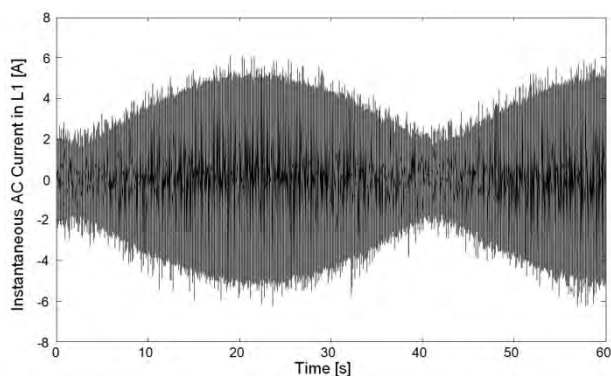

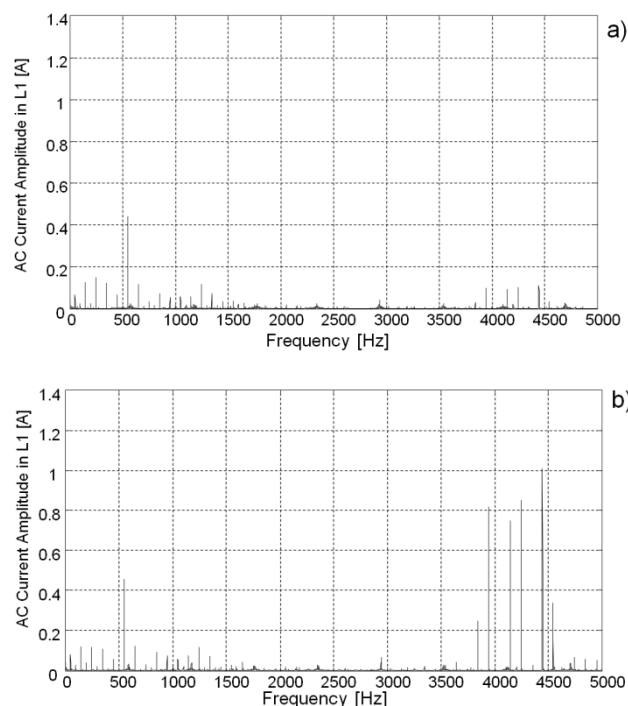Fig. 19. Frequency desynchronization between voltage and current.

Fig. 20. Frequency desynchronization between voltage and current.

5 DC Power Quality Analysis

In Fig. 21 and 22 the time waveforms of voltage and current on strings connected at first MPPT during normal full sun working condition are reported. The spectral analysis corresponding to current is reported in Fig. 23. Higher components are at 50 and 250 Hz but, in general, spectrum presents an unusual harmonic pollution. Different behavior for the string connected to the other MPPT was found. The spectrum of this string is reported in Fig. 24 and a remarkable reduction on harmonic pollution is evident. Reasons of this different behavior are under investigation probably is due to the presence of two stings in parallel.

6 MPPT Analysis

In order to analyze the behavior of the system under non-uniform illuminance conditions, some tests were performed applying a voluntary shade for emulating passage of clouds and analyzing the behavior in terms of voltage and current of both AC and DC side.

A panel inserted in the String 2, connected to MPPT 2 has been completely shaded. Fig.25 and Fig.26 show respectively the voltage and power behaviors during the shading test. In the normal operating conditions voltage is about 580 V and

power about 2040 W. After the shading, voltage reduces to about 550 V and power to about 1850 W. After the intervention of MPPT, voltage increases to about 570 V and power changes to 1830 W. At this working point, the String 1 output power reduces so the MPPT device seems to fail its task. Instead, the whole output power increases because at the new working point the reduction of this string correspond to an higher increment in the other string power output.
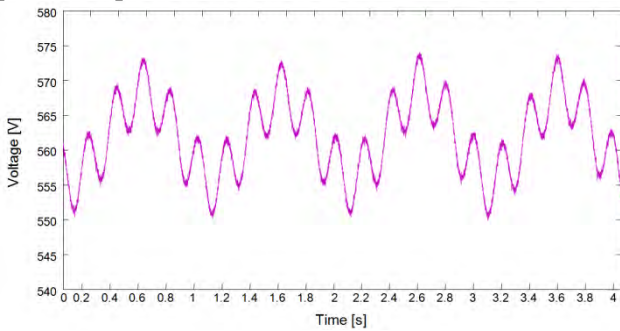

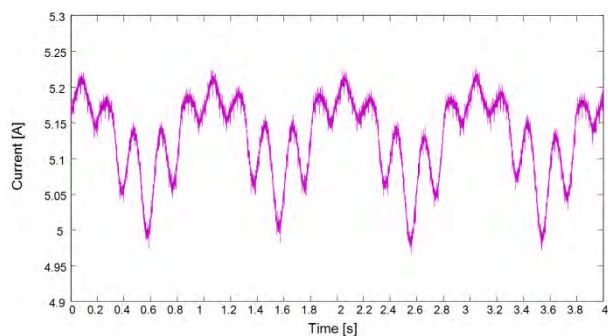Figure 21. Typical voltage DC waveform String 1.

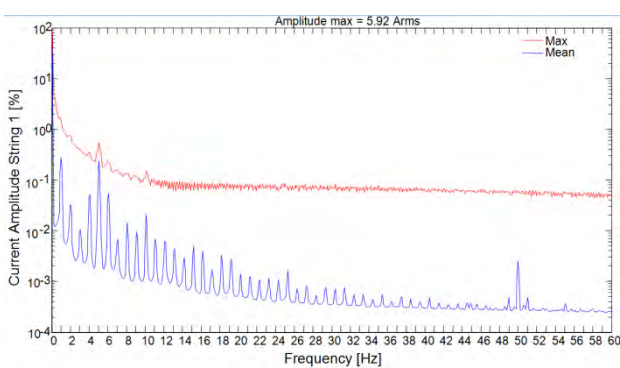Figure 22. Typical waveform of String 1 DC current.

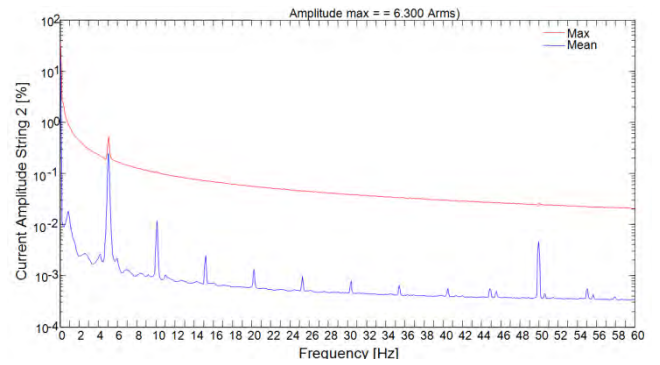Figure 23. Spectrum of String 1 DC current.

Figure 24. Spectrum of String 2 DC current.

7 TRANSIENT EVENT ANALYSIS

The first transient event that applies during measurement campaign is reported in fig. 27: a sudden reduction of supply voltage applied around 5:30. This event is not related with operations of system under analysis. This reduction may be due to a sudden increase of power demand due to the start of the activity of some heavy load in the same area or it is a change of configuration decided by the distributor. This event reflects on the system frequency that begins to oscillate and this behavior lasts for the next two hours. Oscillations are relatively small and power system stability is obviously not compromised. The event has no impact on the energy production of photovoltaic system and frequency oscillation does not affect synchronization of inverter.

Three different transient events are found between 4:30 and 17:00. These events are clearly seen as sudden output power reduction in fig.12. In order to analyze these events the values of DC voltage and current during the same time are reported in Fig. 29. During the event that applies at 17:00, the DC voltage has a little reduction while current has a remarkable reduction. This event probably is due to a partial illumination of PV system for some passing clouds that reduce power generation.

Different events apply at 16:10 and 16:50. During these events the DC voltage has an increment while the current reaches nearly zero values. A little asymmetry in the two strings connected in parallel produces the circulation of a little current (see Fig. 29). This behavior means that the PV strings work openly and the system cannot inject power in the grid. This behavior was related with two dip events in supply voltage that inhibit power injection into the grid.
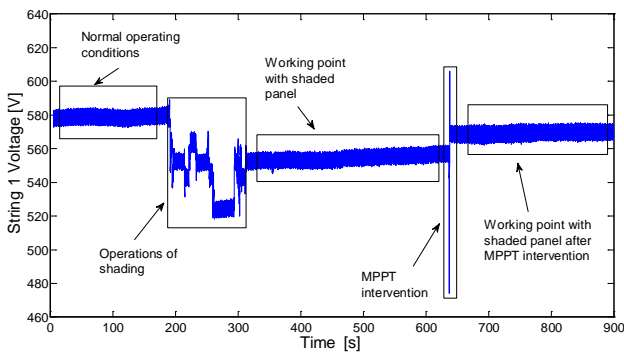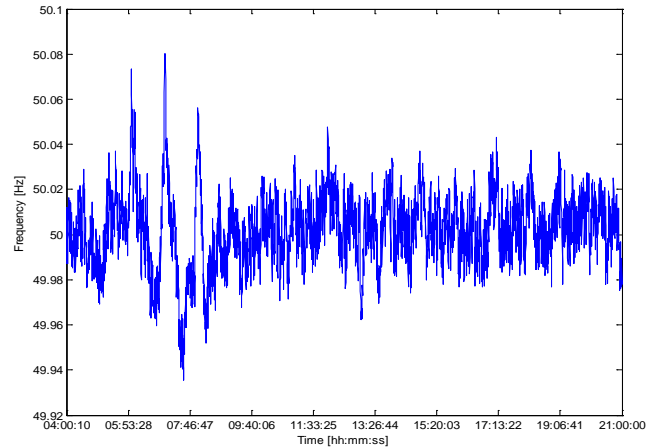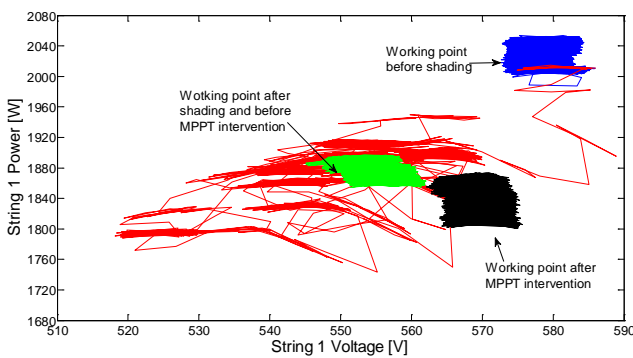
Fig. 25. Voltage behavior during the shading test.

Fig. 26. DC power behavior during shading test.
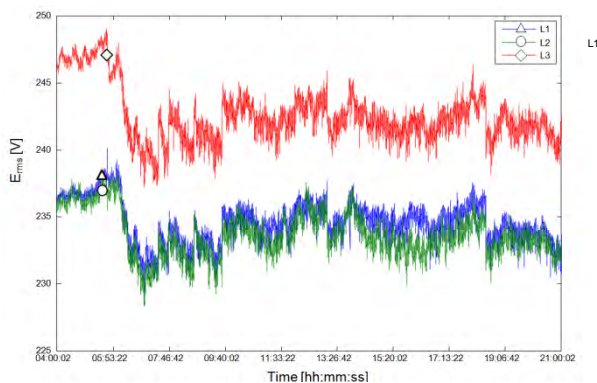
Fig. 27. Line to neutral RMS voltage versus time.

Fig. 28. System frequency versus time.

Fig. 29. DC power behavior during shading test.

8 Conclusion

In this paper some experimental results about power quality issues related with of a photovoltaic system have been presented. In addition to the calculation of common steady state power quality indexes and the comment on them, also transitory situations are analyzed and discussed. An analysis of the electric power components according IEEE 1459 is performed and the results show that, the application of that standard in this practical case presents some critical aspects. The results obtained in this paper could be useful for future works, regarding the construction of a model for energy and malfunctioning forecasting.

References:
[1] IEC EN 50160, "Voltage characteristics of electricity supplied by public distribution systems", 03/2000.

[2] IEEE Standard for Interconnecting Distributed Resources with Electric Power Systems, Std IEEETM-1547, 2003.

[3] IEC EN 61000-3-2, 2005, Electromagnetic compatibility (EMC) - Part 3-2: Limits - Limits for harmonic current emissions

[4] IEEE 1459, 2010, Standard Definitions for the Measurement of Electric Power Quantities Under Sinusoidal, Nonsinusoidal, Balanced or Unbalanced Conditions.

[5] Cataliotti, A.; Cosentino, V.; Nuccio, S.; "The Measurement of Reactive Energy in Polluted Distribution Power Systems: An Analysis of the Performance of Commercial Static Meters", IEEE Transactions on Power Delivery, Volume: 23 , Issue: 3 Year: 2008 , Pg.: 1296 – 1301

[6] Delle Femine, D.Gallo, C.Landi, M. Luiso, "Advanced Instrument for On-Field Calibration of Electrical Energy Meters" IEEE Transactions on Instrumentation and Measurement Vol.58, I.3, March 2009 P: 618 - 625.

[7] S.Orts-Grau, N.Muñoz-Galeano, J.C. Alfonso-Gil, F.J.Gimeno-Sales, S.Seguí-Chilet, "Discussion on Useless Active and Reactive Powers Contained in the IEEE Standard 1459", Transactions on IEEE Power Delivery, Vol.:26 , I.2, 2011 , Page(s): 640 – 649

[8] D. Gallo, C. Landi, M. Luiso, "AC and DC Power Quality of Photovoltaic Systems", Proceedings of IEEE International Instrumentation and Measurement Technology Conference I2MTC 2012, Graz, Austria, 13-16 May 2012, DOI: 10.1109/I2MTC.2012.6229309, Publication Year: 2012 , Page(s): 576 - 581, ISBN: 978-1-4577-1771-0

[9] Papaioannou, I.T.; Bouhouras, A.S.; Marinopoulos, A.G.; Alexiadis, M.C.; Demoulias, C.S.; Labridis, D.P.; "Harmonic impact of small photovoltaic systems connected to the LV distribution network", Electricity Market, 2008. EEM 2008.

[10] A. Delle Femine, D. Gallo, C. Landi, M. Luiso, "Power Quality Monitoring Instrument with FPGA Transducer Compensation", IEEE Transactions on Instrumentation and Measurement, Volume 58, Issue 9, Sept. 2009 Page(s):3149 – 3158.

[11] D. Gallo, C. Landi, M. Luiso, "Accuracy Analysis of Algorithms Adopted in Voltage Dip Measurements", IEEE Transactions on Instrumentation and Measurement, Volume: 59

, Issue: 10 Publication Year: 2010 , Page(s): 2652 – 2659.

[12] L.Asiminoaei, R.Teodorescu, F.Blaabjerg, U.Borup, "Implementation and Test of an Online Embedded Grid Impedance Estimation Technique for PV Inverters" Industrial Electronics, IEEE Transactions on, Volume: 52 , Issue: 4, Page(s): 1136 – 1144

[13] D. Gallo, C. Landi, M. Luiso, "Electrical Signature of Grid Connected Photovoltaic Source: a Preliminary Study" Joint IMEKO TC11 TC19 TC20 International Symposium Cavtat, Croatia, June 15–17, 2011

[14] Ng Jian Liang; G. Kendall, J. Cheng, "Load Signature Study—Part I: Basic Concept, Structure, and Methodology" IEEE Transactions on Power Delivery, Volume: 25, Issue: 2 2010, Page(s): 551 – 560

[15] J.M.Carrasco, L.G. Franquelo, J.T.Bialasiewicz, E.Galvan, R.C.P.Guisado, Ma.A.M. Prats, J.I.Leon, Moreno, N.Alfonso, "Power-Electronic Systems for the Grid Integration of Renewable Energy Sources: A Survey" IEEE Trans. on Industrial Electronics, Vol. 53 , I: 4, 2006 Page(s): 1002 – 1016

[16] Xiao-Qiang Guo, "Real-time measurement method of dc injection for transformerless PV systems", Measurement vol. 44 (2011), pages 1136–1142

[17] M. Aiello; A. Cataliotti; S. Favuzza; G. Graditi, "Theoretical and experimental comparison of total harmonic distortion factors for the evaluation of harmonic and interharmonic pollution of grid-connected photovoltaic systems", Power Delivery, IEEE Transactions on, Volume:21, Issue: 3, 2006 , Page(s): 1390-139

[18] Rikos, E.; Tselepis, S.; Hoyer-Klick, C.; Schroedter-Homscheidt, M., "Stability and Power Quality Issues in Microgrids Under Weather Disturbances", Selected Topics in Applied Earth Observations and Remote Sensing, IEEE Journal of, Volume:1, Issue: 3, 2008 , Page(s): 170- 179

[19] Enslin, J.H.R.; Heskes, P.J.M., "Harmonic interaction between a large number of distributed power inverters and the distribution network", Power Electronics, IEEE Transactions on, Volume:19 , Issue: 6, 2004 , Page(s): 1586 - 1593

[20] Minas Patsalidesa, Andreas Stavroub, Venizelos Efthymioub, George E. Georghiou, "Towards the establishment of maximum PV generation limits due to power quality constraints", International Journal of Electrical

Power & Energy Systems, Volume 42, Issue 1, November 2012, Pages 285–298

[21] Patsalides M, Stavrou A, Georghiou GE. Power quality survey throughout the distribution network in the presence of photovoltaic systems. In: Conference on renewable energy sources and, energy efficiency; 2007. p. 1–8.

[22] Schwaegerl C, Schmitt S., "Distributed energy resources and waveform distortion", In: Conference proceedings: 19th international conference and exhibition on electricity distribution, CIRED, Vienna; May, 2007.

[23] Nakashima E, Miyamoto Y, Fukuoka N, Sugihara H, Tanabe T, Kitamura K., "The characteristics of higher harmonics in clustered PV systems", In: Presented at photovoltaic energy conversion, conference record of the 2006 IEEE 4th World Conference on; 2006.

[24] IEC EN 61000-4-7, 2003, Testing and measurement techniques - General guide on harmonics and interharmonics measurements and instrumentation, for power supply systems and equipment connected thereto.

[25] D.Gallo, R.Langella, A.Testa, "Desynchronized Processing Technique for Harmonic and Interharmonic Analysis", IEEE Transactions on Power Delivery, Vol. 19, I. 3, July 2004, Pages 993-1001.

[26] Si-Hun Jo, SeoEun Son, Jung-Wook Park, "On Improving Distortion Power Quality Index in Distributed Power Grids", Smart Grid, IEEE Transactions on, Volume: 4 , Issue: 1 Publication Year: 2013 , Page(s): 586 – 595

[27] P. K. Ray, S. R. Mohanty, N. Kishor, Classification of Power Quality Disturbances Due to Environmental Characteristics in Distributed Generation System, Sustainable Energy, IEEE Transactions on Volume: 4, Issue: 2, Publication Year: 2013 , Page(s): 302 – 313

[28] M. Castilla, J. Miret, A. Camacho, J. Matas, L. G. de Vicuna, "Reduction of Current Harmonic Distortion in Three-Phase Grid-Connected Photovoltaic Inverters via Resonant Current Control", Industrial Electronics, IEEE Transactions on, Volume: 60, Issue: 4 Publication Year: 2013 , Page(s): 1464 – 1472

[29] D. Gallo, C. Landi, M. Luiso, E. Fiorucci, G. Bucci, F. Ciancetta, "Realization and Characterization of an Electronic Instrument Transducer for MV Networks with Fiber Optic Insulation", WSEAS TRANSACTIONS ON POWER SYSTEMS, ISSN: 1790-5060, E-ISSN: 2224-350X, Issue 1, Volume 8, January 2013

[30] D. Gallo, C. Landi, M. Luiso, E. Fiorucci, G. Bucci, F. Ciancetta, "A Method for Linearization of Optically Insulated Voltage Transducers", WSEAS TRANSACTIONS ON CIRCUITS AND SYSTEMS, ISSN: 1109-2734, E-ISSN: 2224-266X, Issue 3, Volume 12, March 2013

[31] M. Balato, D. Gallo, C. Landi, M. Luiso, M. Vitelli, "Simulation and Laboratory Characterization of a Hybrid MPPT technique based on the Fast Estimate of the Maximum Power Voltages in PV applications", Proceedings of IEEE International Instrumentation and Measurement Technology Conference I2MTC 2013, Minneapolis, MN, USA, 6-9 May 2013

[32] M. Balato, D. Gallo, C. Landi, M. Luiso, M. Vitelli, "Design and Implementation of a Hybrid MPPT technique based on the Scan of the Power vs Voltage input characteristic of the inverter", Proceedings of 19th IMEKO TC 4 Symposium and 17th IWADC Workshop, Advances in Instrumentation and Sensors Interoperability, July 18-19, 2013, Barcelona, Spain